



Exploration of benzofuran-based compounds as potent and selective *Plasmodium falciparum* glycogen synthase kinase-3 (PfGSK-3) inhibitors

Chantalle Moolman^a, Rencia van der Sluis^b, Richard M. Beteck^a, Lesetja J. Legoabe^{a,*}

^a Centre of Excellence for Pharmaceutical Sciences, School of Pharmacy, North-West University, Private Bag X6001, Potchefstroom 2520, South Africa

^b Focus Area for Human Metabolomics, Biochemistry, North-West University, Private Bag X6001, Potchefstroom 2520, South Africa

ARTICLE INFO

Keywords:

Glycogen synthase kinase-3
Plasmodium falciparum
 PfGSK-3
 Malaria
 Protein kinase
 Structure-activity relationship
 Benzofurans

ABSTRACT

Plasmodium falciparum glycogen synthase kinase-3 (PfGSK-3) has been identified as a potential target for the development of novel drugs against multi-drug resistant malaria. A series of benzofuran-based compounds was synthesised and evaluated as inhibitors of recombinantly expressed and purified PfGSK-3 and human glycogen synthase kinase-3 beta (HsGSK-3β). Of this series, five compounds (5k, 5m, 5p, 5r, 5s) preferentially inhibited PfGSK-3, with four of these compounds exhibiting IC₅₀ values in the sub-micromolar range (0.00048–0.440 μM). Evaluation of the structure-activity relationships required for PfGSK-3 selective inhibition indicated that a C6-OCH₃ substitution on ring A is preferred, while the effect of the ring B substituent on activity, in decreasing order is: C4'-CN > C4'-F > C3'-OCH₃ > C3',4'-diCl. To date, development of PfGSK-3 inhibitors has been limited to the 4-phenylthieno[2,3-*b*]pyridine class. Chalcone-based scaffolds, such as the benzofurans described herein, are promising new hits which can be explored for future design of PfGSK-3 selective inhibitors.

1. Introduction

Protein kinases have been exploited as targets for the design and development of small molecules to treat various types of cancers for decades [1,2]. Inspired by the success achieved in oncology, protein kinases are currently being exploited as viable drug targets in other diseases; including diabetes, arthritis and immune disorders [3–5]. The completion of the *Plasmodium falciparum* genome sequencing project in 2002 [6] further stimulated an interest in exploiting the parasite's protein kinases for the development of novel drugs against multi-drug resistant malaria [7–11].

Despite significant progress made in reducing malaria morbidity and mortality over the last decade, this infectious disease continues affecting people worldwide. In 2018, an estimated 228 million malaria cases and 405 000 malaria-related deaths were reported globally [12]. Developing countries, such as sub-Saharan Africa, are more severely affected by malaria due to poverty, limited access to adequate health care and preventative measures, and recurring resistance to insecticides and antimalarial drugs [13]. Sub-Saharan Africa accounted for 93% of all malaria cases and 94% of deaths reported for 2018 [12]. Pregnant women and young children are particularly vulnerable to infection and developing severe malaria, as pregnancy reduces immunity and young

children have not yet acquired partial immunity against the disease. In 2018 alone, a staggering 272 000 children under the age of five, died of this disease [12].

Among the five *Plasmodium* species affecting humans, *P. falciparum* is responsible for the most lethal form of malaria and is also the most prevalent species in sub-Saharan Africa [12]. *P. falciparum* is resistant to several antimalarial drugs including current first-line artemisinin-based combination therapies (ACTs) [14]. Artemisinin resistance is prevalent across Southeast Asia, however, resistance has now also emerged in Rwanda which can significantly compromise malaria control in sub-Saharan Africa [15]. In order to combat multi-drug resistant malaria an urgent need exists to develop new antimalarial drugs with novel modes of action.

Plasmodium kinases are attractive targets for new antimalarial drugs, as they are involved in key signalling pathways throughout the life cycle of the parasite [7]. Of the 65 *Plasmodium* kinases that cluster within known eukaryotic protein kinase families, 36 are considered to be essential for the erythrocytic stages of the parasite [16,17]. *P. falciparum* glycogen synthase kinase-3 (PfGSK-3) is one such essential kinase and has been suggested as a potential drug target [6,18]. PfGSK-3 was identified as one of three GSK-3-related kinases in the *P. falciparum* parasite [17], and shares a high degree of sequence homology with the

* Corresponding author.

E-mail address: Lesetja.Legoabe@nwu.ac.za (L.J. Legoabe).

two human GSK-3 isoforms (*HsGSK-3 α* and *HsGSK-3 β*) [18]. As the crystal structure of *PfGSK-3* is yet to be determined, a tridimensional structure model generated from the *PfGSK-3* sequence and the crystal structure of *HsGSK-3 β* [19], showed a high degree of structural similarity between the two enzymes [18].

As *HsGSK-3* is involved in numerous cellular processes, the extent to which *HsGSK-3* inhibition can be tolerated without presenting unwanted side effects, is still debated on [20–23]. Therefore, inhibitors targeting the plasmodial enzyme would have to be highly selective in order to prevent simultaneous inhibition of *HsGSK-3* and the potential side effects this may cause. Previous studies have tested various established kinase inhibitors such as staurosporine, indirubin-3'-monoxime, hymenialdisine and its derivatives, and members of the paullone family against both enzymes to determine whether *PfGSK-3* selective inhibition would be possible [18,24–26]. The majority of these inhibitors (staurosporine, indirubin-3'-monoxime and hymenialdisine derivatives) were unselective, inhibiting both *PfGSK-3* and mammalian GSK-3 β in the nanomolar range [18,24–26]. However, the paullone inhibitors were more selective towards mammalian GSK-3 β which indicated that species selectivity could be achieved [18,25,26]. Furthermore, certain key structural differences were identified in the active sites of these two enzymes that can be exploited for selective drug design [27,28].

Fugel and co-workers [25] were the first to design a series of novel 3,6-diamino-4-(2-halophenyl)-2-benzoylthieno[2,3-*b*]pyridine-5-carbonitrile derivatives that were highly selective towards *PfGSK-3*. The most active compound of this series (**1**, Fig. 1) inhibited *PfGSK-3* at a sub-micromolar concentration (IC_{50} : 0.48 μ M) and demonstrated *in vitro* antiplasmodial activity (EC_{50} : 5.5 μ M) when tested against the erythrocytic stages of *P. falciparum*. Masch and co-workers [29] further optimised compound **1** by attaching various substituents to the *para* position of the 4-phenyl ring. Compound **2** (Fig. 1) was the most promising of the series as it retained *PfGSK-3* selectivity (*PfGSK-3* IC_{50} : 0.72 μ M; *HsGSK-3 β* IC_{50} : 40.2 μ M), and showed improved aqueous solubility (4.8 μ M) and *in vitro* antiplasmodial activity (EC_{50} : 1.2 μ M) compared to compound **1** (solubility: 1.5 μ M; EC_{50} : 5.5 μ M). The structural core of these inhibitors, 3-amino-4-arylthieno[2,3-*b*]pyridine motif, is based on a well-known chalcone scaffold (highlighted in blue, **1**, Fig. 1). This suggested the potential of using chalcone-like scaffolds in the design of new *PfGSK-3* inhibitors.

Herein we explore an alternative scaffold, benzofurans (**3**, Fig. 1), which is somewhat structurally similar to the thieno[2,3-*b*]pyridine motif. A series of benzofuran-based compounds (**5a-v**) with a variety of polar and lipophilic substituents on both ring A (R_1 , R_2 , R_3) and ring B (R_1' , R_2'), were synthesised and evaluated as potential inhibitors of recombinantly expressed and purified *PfGSK-3* and *HsGSK-3 β* , in order

to gain further insight into the structure-activity relationship around this scaffold for the design of potent and selective *PfGSK-3* inhibitors.

2. Experimental section

2.1. Chemistry

All starting materials for chemical synthesis were purchased from Sigma-Aldrich and used without further purification. Progress of reactions were monitored by thin layer chromatography (TLC) using

Silica gel 60F₂₅₄ aluminium sheets (Merck) and a UV254 fluorescent indicator. The proton (1H) and carbon (^{13}C) nuclear magnetic resonance (NMR) spectra were recorded on a Bruker Avance III 600 spectrometer at frequencies of 600 MHz and 151 MHz, respectively. Either deuterated chloroform ($CDCl_3$) or dimethylsulfoxide ($DMSO-d_6$) was used as solvent and tetramethylsilane (TMS) as internal reference for NMR analysis. All chemical shifts (δ) are reported in parts per million (ppm) in relation to the solvent signal ($CDCl_3$ residual peak at 7.26 ppm and $DMSO-d_6$ residual peak at 2.50 ppm for 1H NMR). Spin multiplicities are reported as follows: s (singlet), d (doublet), dd (doublet of doublets), ddd (doublet of doublets of doublets), t (triplet) and m (multiplet). Coupling constants (J) are reported in Hz. High resolution mass spectra (HRMS) were recorded on a Bruker micrOTOF-Q II mass spectrometer using atmospheric pressure chemical ionisation (APCI) in positive mode. High performance liquid chromatography (HPLC) analyses were done using an Agilent 1100 HPLC system. Melting points (mp) were determined using a Buchi B545 melting point apparatus and values are reported as obtained. Characterisation data for all compounds are available in the [Supplementary material](#).

2.1.1. Synthesis of compounds **3a** and **4a**

2.1.1.1. 2-hydroxy-4,5-dimethoxybenzaldehyde (3a). 2,4,5-Trimethoxybenzaldehyde (15.0 g, 76 mmol) was added to DCM (100 ml) and the mixture was cooled on ice. BBr_3 (19.2 g, 76 mmol) was then added dropwise and the solution was stirred while on ice for approximately 10 min before stirring at room temperature for 5 h. Upon reaction completion as suggested by TLC analysis, the reaction mixture was again cooled on ice and HCl (32%, 40 ml) was slowly added to the mixture while stirring. The resulting precipitate was collected by filtration. The filtrate was extracted with DCM (3x 100 ml), the combined organic extracts were dried over $MgSO_4$ and solvent removed *in vacuo*. The resultant crude from the organic extracts were pooled with the dried precipitate to yield compound **2a** as a dark green solid (2.6 g, 91%), which was used without further purification. mp: 99.8–102.3 $^{\circ}C$; 1H

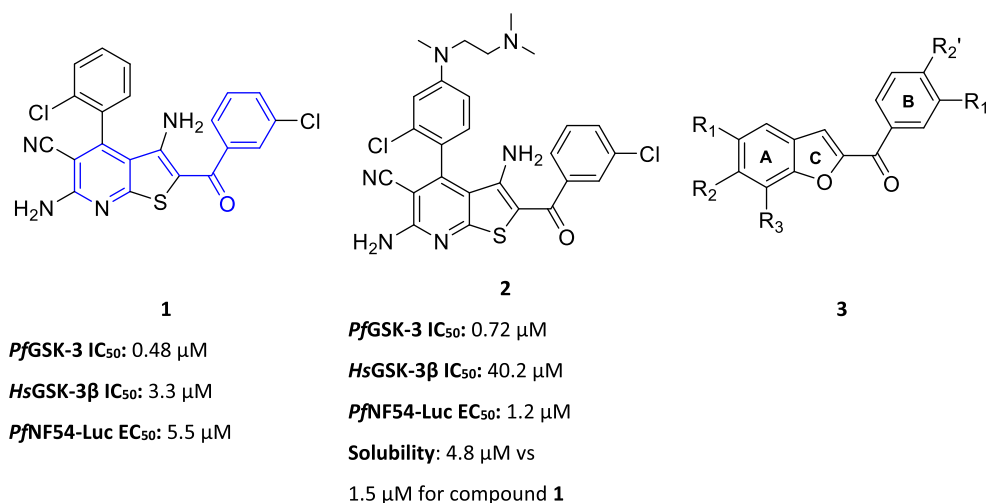


Fig. 1. *PfGSK-3* selective inhibitors (**1** and **2**) belonging to the 4-phenylthieno[2,3-*b*]pyridine class, synthesised by Fugel et al. [25] and Masch et al. [29]. The structural core of these compounds is based on a well-known chalcone scaffold (**1**, highlighted in blue). Another chalcone-based scaffold, benzofurans (**3**), was explored for the design of potent and selective *PfGSK-3* inhibitors during the present study. IC_{50} : half-maximal inhibitory concentration; *PfNF54-Luc*: transgenic *Plasmodium falciparum* NF54 strain expressing the luciferase gene; EC_{50} : half-maximal effective concentration. (For interpretation of the references to colour in this figure legend, the reader is referred to the web version of this article.)

NMR (600 MHz, CDCl₃) δ 11.41 (s, 1H), 9.70 (s, 1H), 6.91 (s, 1H), 6.47 (s, 1H), 3.94 (s, 3H), 3.88 (s, 3H); ¹³C NMR (151 MHz, CDCl₃) δ 194.01, 159.38, 157.26, 142.97, 113.18, 112.88, 100.17, 56.46, 56.38. APCI-HRMS m/z calculated for C₉H₁₁O₄ (MH⁺): 183.0652, found: 183.0667. Purity (HPLC): 90.81%.

2.1.1.2. 2-bromo-3'-methoxyacetophenone (4a). CuBr₂ (14.88 g, 66.62 mmol) was added to a solution of 3'-methoxyacetophenone (5.00 g, 33.29 mmol) in ethyl acetate (75 ml) and DCM (75 ml). The reaction mixture was stirred at 85 °C for 24 h. Upon completion as suggested by TLC analysis, the reaction mixture was cooled to room temperature and then filtered through a bed of silica. The filtrate was concentrated to yield compound **2b** as a green solid (6.98 g, 91%), which was used without further purification. mp: 53.7–54.9 °C; ¹H NMR (600 MHz, DMSO) δ 7.60 (d, J = 7.8 Hz, 1H), 7.50–7.45 (m, 2H), 7.27–7.24 (m, 1H), 4.95 (s, 2H), 3.82 (s, 3H); ¹³C NMR (151 MHz, DMSO) δ 191.57, 159.44, 135.35, 130.04, 121.18, 119.84, 113.28, 55.42, 34.36. APCI-HRMS m/z calculated for C₉H₁₀BrO₂ (MH⁺): 228.9859, found: 228.9862. Purity (HPLC): 56.08%.

2.1.2. Synthesis of compounds 5a-r

2.1.2.1. 1-benzofuran-2-yl(phenyl)methanone (5a). Anhydrous K₂CO₃ (1.70 g, 12.28 mmol) was added to a mixture of 2-bromoacetophenone (0.82 g, 4.09 mmol) and salicylaldehyde (0.44 ml, 4.09 mmol) in PEG-400 (5 ml) and the mixture was stirred at 100 °C. Upon reaction completion as indicated by TLC analysis, the reaction mixture was cooled to room temperature and quenched with deionised water (10 ml). In cases where a precipitate was formed, it was collected by filtration. When no precipitate formed upon addition of water, the mixture was extracted with ethyl acetate (3x 20 ml). The combined organic extracts were washed with brine (20 ml), dried over MgSO₄, concentrated and recrystallized from a suitable solvent [either ethanol (**5a-q**) or methanol (**5r-s**)] to yield the title compound **5a** as a yellow solid (67%): mp: 90.3–91.8 °C; ¹H NMR (600 MHz, CDCl₃) δ 8.08–8.02 (m, 2H), 7.73 (d, J = 7.8 Hz, 1H), 7.68–7.61 (m, 2H), 7.58–7.47 (m, 4H), 7.37–7.31 (m, 1H); ¹³C NMR (151 MHz, CDCl₃) δ 184.44, 156.02, 152.22, 137.25, 132.92, 129.46, 128.56, 128.41, 127.02, 124.01, 123.34, 116.60, 112.60. APCI-HRMS m/z calculated for C₁₅H₁₁O₂ (MH⁺): 223.0754, found: 223.0763. Purity (HPLC): 95.88%.

2.1.2.2. (5-chloro-1-benzofuran-2-yl)(phenyl)methanone (5b). Prepared as for **5a** from 2-bromoacetophenone (0.30 g, 1.51 mmol) and 5-chlorosalicylaldehyde (0.24 g, 1.51 mmol) with anhydrous K₂CO₃ (0.63 g, 4.25 mmol) to yield compound **5b** as white crystals (66%): mp: 142.8–143.3 °C; ¹H NMR (600 MHz, CDCl₃) δ 8.04–7.99 (m, 2H), 7.70–7.60 (m, 2H), 7.58–7.49 (m, 3H), 7.46–7.41 (m, 2H); ¹³C NMR (151 MHz, CDCl₃) δ 184.10, 154.21, 153.30, 136.84, 133.16, 129.60, 129.45, 128.65, 128.61, 128.19, 122.59, 115.45, 113.65. APCI-HRMS m/z calculated for C₁₅H₁₀ClO₂ (MH⁺): 257.0364, found: 257.0364. Purity (HPLC): 99.1%.

2.1.2.3. (7-bromo-5-chloro-1-benzofuran-2-yl)(phenyl)methanone (5c). Prepared as for **5a** from 2-bromoacetophenone (0.30 g, 1.50 mmol) and 3-bromo-5-chlorosalicylaldehyde (0.36 g, 1.50 mmol) with anhydrous K₂CO₃ (0.63 g, 4.25 mmol) to yield compound **5c** as dark beige crystals (43%): mp: 143.4–144.5 °C; ¹H NMR (600 MHz, CDCl₃) δ 8.12–8.07 (m, 2H), 7.67–7.59 (m, 3H), 7.57–7.51 (m, 3H); ¹³C NMR (151 MHz, CDCl₃) δ 183.25, 154.10, 151.71, 136.37, 133.42, 130.82, 130.04, 129.69, 129.46, 128.66, 121.69, 115.30, 105.61. APCI-HRMS m/z calculated for C₁₅H₉BrClO₂ (MH⁺): 334.9469, found: 334.9465. Purity (HPLC): 97.35%.

2.1.2.4. (5-chloro-1-benzofuran-2-yl)(4-chlorophenyl)methanone (5d). Prepared as for **5a** from 2,4'-dichloroacetophenone (0.30 g, 1.59 mmol)

and 5-chlorosalicylaldehyde (0.25 g, 1.59 mmol) with anhydrous K₂CO₃ (0.66 g, 4.76 mmol) to yield compound **5d** as white crystals (66%): mp: 191.3–191.8 °C; ¹H NMR (600 MHz, CDCl₃) δ 8.03–7.96 (m, 2H), 7.69 (d, J = 2.0 Hz, 1H), 7.57–7.41 (m, 5H); ¹³C NMR (151 MHz, CDCl₃) δ 182.64, 154.21, 153.18, 139.74, 134.99, 130.93, 129.76, 128.97, 128.84, 128.09, 122.63, 115.38, 113.64. APCI-HRMS m/z calculated for C₁₅H₉Cl₂O₂ (MH⁺): 290.9974, found: 290.9963. Purity (HPLC): 100%.

2.1.2.5. (7-bromo-5-chloro-1-benzofuran-2-yl)(4-chlorophenyl)methanone (5e). Prepared as for **5a** from 2,4'-dichloroacetophenone (0.30 g, 1.59 mmol) and 3-bromo-5-chlorosalicylaldehyde (0.37 g, 1.59 mmol) with anhydrous K₂CO₃ (0.66 g, 4.76 mmol) to yield compound **5e** as beige crystals (42%): mp: 164.9–165.0 °C; ¹H NMR (600 MHz, CDCl₃) δ 8.12–8.07 (m, 2H), 7.64 (q, J = 1.8 Hz, 2H), 7.57 (s, 1H), 7.52 (d, J = 8.5 Hz, 2H); ¹³C NMR (151 MHz, CDCl₃) δ 181.81, 153.99, 151.69, 140.08, 134.51, 131.19, 130.97, 130.20, 129.04, 128.55, 121.73, 115.26, 105.58. APCI-HRMS m/z calculated for C₁₅H₈BrCl₂O₂ (MH⁺): 368.9079, found: 368.9052. Purity (HPLC): 99.76%.

2.1.2.6. 1-benzofuran-2-yl(4-chlorophenyl)methanone (5f). Prepared as for **5a** from 2,4'-dichloroacetophenone (0.30 g, 1.59 mmol) and salicylaldehyde (0.17 ml, 1.59 mmol) with anhydrous K₂CO₃ (0.66 g, 4.76 mmol) to yield compound **5f** as beige crystals (65%): mp: 150.0–151.4 °C; ¹H NMR (600 MHz, CDCl₃) δ 8.10–7.98 (m, 2H), 7.72 (d, J = 7.7 Hz, 1H), 7.62 (d, J = 8.3 Hz, 1H), 7.60–7.46 (m, 4H), 7.33 (t, J = 7.4 Hz, 1H); ¹³C NMR (151 MHz, CDCl₃) δ 182.94, 155.99, 152.04, 139.42, 135.36, 130.91, 128.87, 128.55, 126.87, 124.09, 123.34, 116.48, 112.54. APCI-HRMS m/z calculated for C₁₅H₁₀ClO₂ (MH⁺): 257.0364, found: 257.0339. Purity (HPLC): 100%.

2.1.2.7. [6-(diethylamino)benzofuran-2-yl](phenyl)methanone hydrochloride (5g). [6-(diethylamino)benzofuran-2-yl](phenyl)methanone was prepared as for **5a** from 2-bromoacetophenone (0.52 g, 2.59 mmol) and 4-(diethylamino)salicylaldehyde (0.5 g, 2.59 mmol) with anhydrous K₂CO₃ (1.07 g, 7.76 mmol) to yield a yellow oil. The oil was dissolved in ethanol (10 ml), and acetyl chloride (5 ml) was added dropwise to the mixture while stirring at room temperature. The title compound (**5g**) was collected by filtration as a yellow solid (50%): mp: 215.4–217.1 °C; ¹H NMR (600 MHz, CDCl₃) δ 8.26 (s, 1H), 8.12–8.07 (m, 2H), 7.93 (d, J = 8.5 Hz, 1H), 7.81 (dd, J = 8.4, 1.1 Hz, 1H), 7.68 (dd, J = 10.6, 4.3 Hz, 1H), 7.63 (s, 1H), 7.57 (t, J = 7.8 Hz, 2H), 3.63 (d, J = 7.2 Hz, 4H), 1.32 (t, J = 7.2 Hz, 6H); ¹³C NMR (151 MHz, CDCl₃) δ 183.58, 155.20, 154.82, 136.95, 136.30, 133.59, 129.65, 128.76, 128.42, 125.17, 118.63, 114.90, 108.29, 54.07, 10.44. APCI-HRMS m/z calculated for C₁₉H₂₀NO₂ (MH⁺): 294.1489, found: 294.1517. Purity (HPLC): 100%.

2.1.2.8. (4-chlorophenyl)(7-methoxy-1-benzofuran-2-yl)methanone (5h). Prepared as for **5a** from 2,4'-dichloroacetophenone (0.50 g, 2.64 mmol) and *o*-vanillin (0.40 g, 2.64 mmol) with anhydrous K₂CO₃ (1.10 g, 7.93 mmol) to yield compound **5h** as beige crystals (82%): mp: 189.9–190.5 °C; ¹H NMR (600 MHz, CDCl₃) δ 8.08–8.03 (m, 2H), 7.55 (s, 1H), 7.53–7.48 (m, 2H), 7.27 (ddd, J = 15.7, 10.5, 4.4 Hz, 2H), 6.96 (dd, J = 7.8, 0.8 Hz, 1H), 4.02 (s, 3H); ¹³C NMR (151 MHz, CDCl₃) δ 182.56, 152.45, 146.08, 145.72, 139.42, 135.26, 131.06, 128.87, 128.49, 124.75, 116.27, 114.97, 109.63, 56.07. APCI-HRMS m/z calculated for C₁₆H₁₂ClO₃ (MH⁺): 287.0469, found: 287.0473. Purity (HPLC): 100%.

2.1.2.9. (4-chlorophenyl)(6-methoxy-1-benzofuran-2-yl)methanone (5i). Prepared as for **5a** from 2,4'-dichloroacetophenone (0.50 g, 2.64 mmol) and 2-hydroxy-4'-methoxybenzaldehyde (0.40 g, 2.64 mmol) with anhydrous K₂CO₃ (1.10 g, 7.93 mmol) to yield compound **5i** as pink crystals (54%): mp: 186.7–187.4 °C; ¹H NMR (600 MHz, CDCl₃) δ 7.98–7.93 (m, 2H), 7.56 (d, J = 8.7 Hz, 1H), 7.50–7.44 (m, 3H), 7.07 (d, J = 1.9 Hz, 1H), 6.95 (dd, J = 8.7, 2.2 Hz, 1H), 3.87 (s, 3H); ¹³C NMR

(151 MHz, CDCl₃) δ 182.42, 161.37, 157.68, 151.62, 139.05, 135.71, 130.74, 128.80, 123.67, 120.24, 117.26, 114.70, 95.54, 55.74. APCI-HRMS m/z calculated for C₁₆H₁₂ClO₃ (MH⁺): 287.0469, found: 287.0498. Purity (HPLC): 100%.

2.1.2.10. (4-chlorophenyl)(5-methoxy-1-benzofuran-2-yl)methanone (5j). Prepared as for **5a** from 2,4'-dichloroacetophenone (0.30 g, 1.59 mmol) and 2-hydroxy-5'-methoxybenzaldehyde (0.20 ml, 1.59 mmol) with anhydrous K₂CO₃ (0.66 g, 4.76 mmol) to yield compound **5j** as pink crystals (65%): mp: 190.6–191.1 °C; ¹H NMR (600 MHz, CDCl₃) δ 8.04–7.97 (m, 2H), 7.53–7.46 (m, 4H), 7.14–7.07 (m, 2H), 3.84 (s, 3H); ¹³C NMR (151 MHz, CDCl₃) δ 182.78, 156.71, 152.78, 151.22, 139.36, 135.38, 130.94, 128.85, 127.39, 118.78, 116.45, 113.22, 103.83, 55.84. APCI-HRMS m/z calculated for C₁₆H₁₂ClO₃ (MH⁺): 287.0469, found: 287.0499. Purity (HPLC): 100%.

2.1.2.11. (3,4-dichlorophenyl)(6-methoxy-1-benzofuran-2-yl)methanone (5k). Prepared as for **5a** from 2-bromo-3',4'-dichloroacetophenone (0.88 g, 3.29 mmol) and 2-hydroxy-4'-methoxybenzaldehyde (0.50 g, 3.29 mmol) with anhydrous K₂CO₃ (1.36 g, 9.86 mmol) to yield compound **5k** as brown crystals (52%): mp: 162.5–163.7 °C; ¹H NMR (600 MHz, DMSO) δ 8.21 (d, J = 2.0 Hz, 1H), 8.00 (dd, J = 8.3, 2.0 Hz, 1H), 7.93 (d, J = 8.3 Hz, 1H), 7.88 (s, 1H), 7.80 (d, J = 8.7 Hz, 1H), 7.44 (d, J = 1.6 Hz, 1H), 7.09 (dd, J = 8.7, 1.6 Hz, 1H), 3.93 (s, 3H); ¹³C NMR (151 MHz, DMSO) δ 180.89, 161.78, 157.80, 150.95, 137.77, 136.00, 132.14, 131.50, 131.23, 129.58, 124.91, 120.51, 119.20, 115.19, 96.23, 56.39. APCI-HRMS m/z calculated for C₁₆H₁₁Cl₂O₃ (MH⁺): 321.0080, found: 321.0062. Purity (HPLC): 100%.

2.1.2.12. (6-methoxy-1-benzofuran-2-yl)(phenyl)methanone (5l). Prepared as for **5a** from 2-bromoacetophenone (0.65 g, 3.29 mmol) and 2-hydroxy-4'-methoxybenzaldehyde (0.50 g, 3.29 mmol) with anhydrous K₂CO₃ (1.36 g, 9.86 mmol) to yield compound **5l** as beige crystals (57%): mp: 103.8–104.6 °C; ¹H NMR (600 MHz, CDCl₃) δ 8.00–7.96 (m, 2H), 7.62–7.47 (m, 4H), 7.44 (d, J = 0.7 Hz, 1H), 7.08 (d, J = 1.9 Hz, 1H), 6.94 (dd, J = 8.7, 2.2 Hz, 1H), 3.87 (s, 3H); ¹³C NMR (151 MHz, CDCl₃) δ 183.90, 161.23, 157.65, 151.80, 137.53, 132.58, 129.26, 128.46, 123.63, 120.34, 117.33, 114.53, 95.59, 55.72. APCI-HRMS m/z calculated for C₁₆H₁₃O₃ (MH⁺): 253.0859, found: 253.0861. Purity (HPLC): 100%.

2.1.2.13. (4-fluorophenyl)(6-methoxy-1-benzofuran-2-yl)methanone (5m). Prepared as for **5a** from 2-bromo-4'-fluoroacetophenone (0.71 g, 3.29 mmol) and 2-hydroxy-4'-methoxybenzaldehyde (0.50 g, 3.29 mmol) with anhydrous K₂CO₃ (1.36 g, 9.86 mmol) to yield compound **5m** as a light brown solid (90%): mp: 161.1–163.1 °C; ¹H NMR (600 MHz, CDCl₃) δ 8.11–8.05 (m, 2H), 7.58 (d, J = 8.7 Hz, 1H), 7.48 (d, J = 0.9 Hz, 1H), 7.24–7.18 (m, 2H), 7.10 (d, J = 1.9 Hz, 1H), 6.97 (dd, J = 8.7, 2.2 Hz, 1H), 3.90 (s, 3H); ¹³C NMR (151 MHz, CDCl₃) δ 182.22, 165.52 (d, J = 254.3 Hz), 161.32, 157.66, 151.79, 133.70 (d, J = 3.1 Hz), 131.97 (d, J = 9.1 Hz), 123.66, 120.31, 117.08, 115.68 (d, J = 21.8 Hz), 114.67, 95.61, 55.77. APCI-HRMS m/z calculated for C₁₆H₁₂FO₃ (MH⁺): 271.0765, found: 271.0743. Purity (HPLC): 98.28%.

2.1.2.14. (4-bromophenyl)(6-methoxy-1-benzofuran-2-yl)methanone (5n). Prepared as for **5a** from 2,4'-dibromoacetophenone (0.91 g, 3.29 mmol) and 2-hydroxy-4'-methoxybenzaldehyde (0.50 g, 3.29 mmol) with anhydrous K₂CO₃ (1.36 g, 9.86 mmol) to yield compound **5n** as a light brown solid (85%): mp: 200.9–202.4 °C; ¹H NMR (600 MHz, CDCl₃) δ 7.94–7.87 (m, 2H), 7.71–7.61 (m, 2H), 7.59 (d, J = 8.7 Hz, 1H), 7.48 (d, J = 0.9 Hz, 1H), 7.10 (d, J = 1.9 Hz, 1H), 6.98 (dd, J = 8.7, 2.2 Hz, 1H), 3.90 (s, 3H); ¹³C NMR (151 MHz, CDCl₃) δ 182.60, 161.43, 157.74, 151.63, 136.19, 131.82, 130.88, 127.71, 123.72, 120.28, 117.34, 114.76, 95.59, 55.79. APCI-HRMS m/z calculated for C₁₆H₁₂BrO₃ (MH⁺): 330.9964, found: 330.9965. Purity (HPLC):

96.52%.

2.1.2.15. (6-methoxy-1-benzofuran-2-yl)(4-methoxyphenyl)methanone (5o). Prepared as for **5a** from 2-bromo-4'-methoxyacetophenone (0.75 g, 3.29 mmol) and 2-hydroxy-4'-methoxybenzaldehyde (0.50 g, 3.29 mmol) with anhydrous K₂CO₃ (1.36 g, 9.86 mmol) to yield compound **5o** as a beige solid (86%): mp: 151.0–151.3 °C; ¹H NMR (600 MHz, CDCl₃) δ 8.12–8.03 (m, 2H), 7.57 (d, J = 8.7 Hz, 1H), 7.46 (d, J = 0.7 Hz, 1H), 7.10 (d, J = 1.9 Hz, 1H), 7.04–6.93 (m, 3H), 3.90 (d, J = 9.5 Hz, 6H); ¹³C NMR (151 MHz, CDCl₃) δ 182.46, 163.38, 160.97, 157.42, 152.25, 131.76, 130.13, 123.48, 120.42, 116.25, 114.34, 113.79, 95.67, 55.75, 55.53. APCI-HRMS m/z calculated for C₁₇H₁₅O₄ (MH⁺): 283.0965, found: 283.0974. Purity (HPLC): 100%.

2.1.2.16. 4-[(6-methoxy-1-benzofuran-2-yl)carbonyl]benzonitrile (5p). Prepared as for **5a** from 2-bromo-4'-cyanoacetophenone (0.74 g, 3.29 mmol) and 2-hydroxy-4'-methoxybenzaldehyde (0.50 g, 3.29 mmol) with anhydrous K₂CO₃ (1.36 g, 9.86 mmol) to yield compound **5p** as a beige solid (80%): mp: 183.1–186.7 °C; ¹H NMR (600 MHz, CDCl₃) δ 8.14–8.08 (m, 2H), 7.86–7.80 (m, 2H), 7.60 (d, J = 8.7 Hz, 1H), 7.52 (d, J = 0.9 Hz, 1H), 7.09 (d, J = 1.9 Hz, 1H), 6.99 (dd, J = 8.7, 2.2 Hz, 1H), 3.91 (s, 3H); ¹³C NMR (151 MHz, CDCl₃) δ 181.93, 161.81, 158.00, 151.27, 140.93, 132.32, 129.76, 123.91, 120.18, 118.09, 118.02, 115.88, 115.12, 95.53, 55.82. APCI-HRMS m/z calculated for C₁₇H₁₂NO₃ (MH⁺): 278.0812, found: 278.0801. Purity (HPLC): 98.24%.

2.1.2.17. (4-chlorophenyl)(5,6-dimethoxy-1-benzofuran-2-yl)methanone (5q). Prepared as for **5a** from 2,4'-dichloroacetophenone (0.52 g, 2.74 mmol) and compound **3a** (0.50 g, 2.74 mmol) with anhydrous K₂CO₃ (1.14 g, 8.23 mmol) to yield compound **5q** as white crystals (85%): mp: 183.8–184.0 °C; ¹H NMR (600 MHz, CDCl₃) δ 8.01–7.97 (m, 2H), 7.54–7.46 (m, 3H), 7.11 (s, 1H), 7.07 (s, 1H), 3.98 (s, 3H), 3.95 (s, 3H); ¹³C NMR (151 MHz, CDCl₃) δ 182.06, 152.03, 151.98, 151.78, 147.94, 139.00, 135.81, 130.82, 128.79, 119.09, 117.34, 102.69, 95.13, 56.36, 56.35. APCI-HRMS m/z calculated for C₁₇H₁₄ClO₄ (MH⁺): 317.0575, found: 317.0574. Purity (HPLC): 100%.

2.1.2.18. (6-Methoxybenzofuran-2-yl)(3-methoxyphenyl)methanone (5r). Prepared as for **5a** from compound **4a** (0.75 g, 3.29 mmol) and 2-hydroxy-4-methoxybenzaldehyde (0.50 g, 3.29 mmol) with anhydrous K₂CO₃ (1.36 g, 9.86 mmol) to yield compound **5r** as a light grey solid (52%): mp: 81.4–81.5 °C; ¹H NMR (600 MHz, CDCl₃) δ 7.58 (dd, J = 14.9, 8.1 Hz, 2H), 7.50 (s, 1H), 7.47 (s, 1H), 7.43 (t, J = 7.9 Hz, 1H), 7.18–7.14 (m, 1H), 7.10 (s, 1H), 6.96 (dd, J = 8.6, 2.0 Hz, 1H), 3.89 (m, 6H); ¹³C NMR (151 MHz, CDCl₃) δ 183.77, 161.43, 159.81, 157.84, 151.93, 138.96, 129.61, 123.80, 121.99, 120.50, 119.09, 117.54, 114.70, 114.01, 95.79, 55.90, 55.66. APCI-HRMS m/z calculated for C₁₇H₁₅O₄ (MH⁺): 283.0965, found: 283.0946. Purity (HPLC): 99.40%.

2.1.2.19. (7-Methoxybenzofuran-2-yl)(3-methoxyphenyl)methanone (5s). Prepared as for **5a** from 2-hydroxy-3-methoxybenzaldehyde (0.50 g, 3.29 mmol) and compound **4a** (0.75 g, 3.29 mmol) with anhydrous K₂CO₃ (1.36 g, 9.86 mmol) to yield compound **5s** as a brown solid (46%): mp: 80.1–86.8 °C; ¹H NMR (600 MHz, CDCl₃) δ 7.81–7.73 (m, 1H), 7.66 (d, J = 0.8 Hz, 1H), 7.62 (t, J = 6.7 Hz, 1H), 7.57–7.48 (m, 1H), 7.44–7.29 (m, 3H), 7.05 (dd, J = 13.0, 7.0 Hz, 1H), 4.12 (s, 3H), 3.97 (s, 3H); ¹³C NMR (151 MHz, CDCl₃) δ 183.83, 159.83, 152.65, 146.29, 145.92, 138.53, 129.66, 128.76, 124.78, 122.35, 119.61, 116.56, 115.14, 114.03, 109.83, 56.30, 55.64. APCI-HRMS m/z calculated for C₁₇H₁₅O₄ (MH⁺): 283.0965, found: 283.0970. Purity (HPLC): 98.03%.

2.1.3. Synthesis of compounds 5t-v

2.1.3.1. (4-chlorophenyl)(7-hydroxy-1-benzofuran-2-yl)methanone (5t).

AlCl_3 (0.87 g, 6.49 mmol) was added to a 100 ml round bottom flask containing **5h** (0.62 g, 2.17 mmol) and toluene (5 ml). The mixture was stirred at 100 °C. Upon reaction completion as suggested by TLC analysis, the mixture was cooled to room temperature and quenched with deionised water (10 ml). The mixture was then extracted with ethyl acetate (3x 20 ml). The combined organic extracts were washed with brine (20 ml), dried over MgSO_4 , concentrated and purified using silica gel column chromatography (petroleum ether: ethyl acetate, 5:1) to yield compound **5t** as a beige solid (29%); mp: 213.4–214.5 °C; ^1H NMR (600 MHz, DMSO) δ 10.42 (s, 1H), 8.06–7.99 (m, 2H), 7.76 (s, 1H), 7.70–7.63 (m, 2H), 7.24 (dd, $J = 7.8, 1.0$ Hz, 1H), 7.16 (t, $J = 7.8$ Hz, 1H), 6.97 (dd, $J = 7.7, 1.0$ Hz, 1H); ^{13}C NMR (151 MHz, DMSO) δ 182.29, 151.05, 144.88, 143.32, 137.97, 135.45, 131.13, 128.86, 128.61, 124.96, 117.75, 114.02, 113.81. APCI-HRMS m/z calculated for $\text{C}_{15}\text{H}_{10}\text{ClO}_3$ (MH^+): 273.0313, found: 273.0304. Purity (HPLC): 98.58%.

2.1.3.2. (4-chlorophenyl)(6-hydroxy-1-benzofuran-2-yl)methanone

(**5u**). Prepared as for **5s** from compound **5i** (0.41 g, 1.43 mmol) with AlCl_3 (0.57 g, 4.28 mmol) to yield compound **5u** as a beige solid (27%); mp: 212.2–212.9 °C; ^1H NMR (600 MHz, DMSO) δ 10.27 (s, 1H), 7.99–7.95 (m, 2H), 7.71 (d, $J = 0.8$ Hz, 1H), 7.68–7.62 (m, 3H), 7.06–7.02 (m, 1H), 6.91 (dd, $J = 8.6, 2.1$ Hz, 1H); ^{13}C NMR (151 MHz, DMSO) δ 181.98, 160.02, 157.78, 150.73, 138.01, 136.33, 131.32, 129.25, 124.95, 119.49, 118.99, 115.23, 97.95. APCI-HRMS m/z calculated for $\text{C}_{15}\text{H}_{10}\text{ClO}_3$ (MH^+): 273.0313, found: 273.0326. Purity (HPLC): 100%.

2.1.3.3. (4-chlorophenyl)(5-hydroxy-1-benzofuran-2-yl)methanone

(**5v**). Prepared as for **5s** from compound **5j** (0.28 g, 0.96 mmol) with AlCl_3 (0.39 g, 2.89 mmol) to yield compound **5v** as a yellow solid (29%); mp: 215.8–217.1 °C; ^1H NMR (600 MHz, DMSO) δ 9.57 (s, 1H), 8.04–7.98 (m, 2H), 7.71–7.64 (m, 3H), 7.58 (d, $J = 8.9$ Hz, 1H), 7.12 (d, $J = 2.4$ Hz, 1H), 7.04 (dd, $J = 8.9, 2.5$ Hz, 1H); ^{13}C NMR (151 MHz, DMSO) δ 182.65, 154.64, 152.16, 150.32, 138.34, 135.99, 131.51, 129.30, 128.08, 119.11, 117.69, 113.21, 107.23. APCI-HRMS m/z calculated for $\text{C}_{15}\text{H}_{10}\text{ClO}_3$ (MH^+): 273.0313, found: 273.0309. Purity (HPLC): 95.49%.

2.2. Biology

2.2.1. Cloning of *HsGSK-3 β* and *PfGSK-3*

The full length open reading frame of *HsGSK-3 β* (1263 bp; Ensembl Genome ID: ENST00000264235.12) and *PfGSK-3* (1323 bp; Ensembl Genome ID: PF3D7_0312400) gene sequences were purchased from GeneArt (Thermo Scientific, Waltham, MA). The *HsGSK-3 β* and *PfGSK-3* sequences are available in the [Supplementary material](#) (Figure A and B).

The *HsGSK-3 β* gene was subcloned into the pET32a(+) expression vector using restriction enzyme directional cloning and verified by Sanger sequencing. Purified plasmid DNA was used to transform *Origami*TM cells (Novagen, Madison, WI) already containing the pGro7 chaperone expression plasmid (Takara, Madison, WI).

The *PfGSK-3* gene was amplified by PCR using 5'-ATG AAA AAT TGG CCT-3' as the forward primer and 5'-ACT TTC TAT GAT AAC GTG CGT-3' as the reverse primer (IDT, Coralville, IA). Amplification reactions were prepared according to the PlatinumTM Taq DNA polymerase (Invitrogen, Carlsbad, CA) instruction manual (annealing step: 51.6 °C for 30 s; total of 30 PCR cycles). The *PfGSK-3* gene was then cloned into the pBAD/Thio-TOPO[®] expression vector (pBAD/TOPO[®] ThioFusionTM Expression Kit; Invitrogen, Carlsbad, CA), by direct insertion of the PCR product. The cloning reaction was transformed into chemically competent TOP10 One Shot[®] *E. coli* cells included in the kit. The orientation of the inserts and the fidelity of the constructs were verified by Sanger sequencing.

2.2.2. Expression of recombinant *HsGSK-3 β* and *PfGSK-3*

A single colony of *Origami*TM cells co-transformed with the pGro7 and pET32a(+)-*HsGSK-3 β* plasmids, was inoculated into 5 ml of LB medium with carbenicillin (50 $\mu\text{g}/\text{ml}$) and chloramphenicol (20 $\mu\text{g}/\text{ml}$). The culture was incubated overnight at 37 °C and 225 rpm. The overnight culture was transferred into 100 ml of LB medium with carbenicillin (50 $\mu\text{g}/\text{ml}$), chloramphenicol (20 $\mu\text{g}/\text{ml}$), and 0.5 mg/ml L-arabinose (for expression of the pGro7 chaperone proteins). The culture was incubated at 37 °C and 225 rpm, until an OD_{600} of ± 0.5 was reached. Expression of the *HsGSK-3 β* protein was then induced with 1 mM IPTG for 4 h at 30 °C and 225 rpm.

A single colony of TOP10 *E. coli* transformed with pBAD/Thio-*PfGSK-3* was inoculated into 5 ml of LB medium containing carbenicillin (100 $\mu\text{g}/\text{ml}$). The culture was incubated overnight at 37 °C and 225 rpm. The overnight culture was transferred into 500 ml of LB medium with carbenicillin (100 $\mu\text{g}/\text{ml}$) and cultured at 37 °C and 225 rpm, until an OD_{600} of ± 0.5 was reached. Expression was then induced with 0.02% L-arabinose for 3 h at 37 °C and 225 rpm.

2.2.3. Extraction and purification of recombinant *HsGSK-3 β* and *PfGSK-3*

Bacterial cells were harvested by centrifugation (5000 xg, 10 min, room temperature) and the proteins were extracted using B-PERTM Complete Bacterial Protein Extraction Reagent (Thermo Fisher Scientific, Waltham, MA) according to the supplier's procedure. Briefly, the bacterial pellet was resuspended in the required amount of B-PERTM Reagent (with added protease inhibitors; Complete Ultra Protease Inhibitor Mini Tablets; Merck, Darmstadt, Germany), and incubated at room temperature with gentle rocking for 15 min. The lysate was then centrifuged (16 000 xg, 20 min, 4 °C) and the soluble fraction collected for purification. The recombinant His-tag proteins were then purified by immobilized metal affinity chromatography using Protino[®] Ni-TED 2000 Packed Columns (Macherey-Nagel Inc., Düren, Germany). Briefly, the entire soluble protein fraction was loaded onto a pre-equilibrated column. For the *HsGSK-3 β* protein, the column was washed twice with LEW buffer, before eluting the protein with Elution buffer (250 mM imidazole). For the *PfGSK-3* protein, the column was washed once with LEW buffer and then three times with diluted Elution buffer (5 mM imidazole), before eluting the protein with Elution buffer (250 mM imidazole, 5% glycerol).

Amicon[®] Ultra-15 centrifugal devices with a 50 kDa molecular weight cut-off (Merck, Darmstadt, Germany), were used for further purification and concentration of both recombinant proteins, as well as for exchanging the elution buffer with storage buffer. Storage buffer consisted of 50 mM Tris-HCl pH 8.0 (with added protease inhibitors, Complete Ultra Protease Inhibitor Mini Tablets, Roche); 150 mM NaCl; 0.5 mM EDTA; 0.25 mM DTT; 25% glycerol. SDS-PAGE analysis with Coomassie brilliant blue staining was used to monitor the expression and purification procedures. To confirm the presence of the His-tag proteins, western blot analysis was performed using a 6x His-tag monoclonal antibody (Thermo Fisher Scientific, Madison, WI). Protein concentrations were determined using the Qubit[®] protein assay kit (Life Technologies, Carlsbad, CA) with the Qubit[®] 2.0 fluorometer. Both recombinant proteins were stored in aliquots at –80 °C.

2.2.4. ADP-GloTM kinase assay

Activity of the recombinant *HsGSK-3 β* and *PfGSK-3* were measured using the ADP-GloTM Kinase Assay Kit (Promega, Madison, WI). The assay was optimised by determining the optimal substrate (GS-1 peptide: YRRAAVPPSPSLSRHSSPHQpSEDEEE, where pS is a phosphorylated serine; GenScript, Piscataway, NJ) and enzyme concentrations to use for each reaction. To determine the optimal substrate concentration, serial twofold dilutions of substrate in kinase reaction buffer (40 mM Tris-HCl pH 8.0; 20 mM MgCl_2 ; 0.1 mg/ml BSA; 50 μM DTT) were made, and the reactions were performed using 30 ng of enzyme and 10 μM of ATP per 30 μl reaction. The control reactions consisted of the same serial dilutions of substrate but without any added enzyme. The optimal

substrate concentrations were calculated to be 0.8 mg/ml for *HsGSK-3 β* and 0.6 mg/ml for *PfGSK-3*, as these concentrations resulted in the largest difference in luminescence between the reaction wells and the control wells. To determine the optimal enzyme concentration, serial twofold dilutions of enzyme in kinase reaction buffer were made, and the reactions were performed using the optimal concentration of substrate and 10 μ M of ATP per 20 μ l reaction. The optimal enzyme concentration was within the linear range of the kinase titration curve (luminescence vs enzyme concentration) and generated a signal-to-background ratio of 10 (luminescence of reaction/ luminescence of reaction without kinase). The optimal enzyme concentrations were 8 ng and 32 ng for *HsGSK-3 β* and *PfGSK-3*, respectively.

All test compounds were screened at a concentration of 10 μ M (1% final DMSO concentration). The compounds were dissolved in 100% DMSO, diluted with kinase reaction buffer, and incubated with the kinase for 10 min at room temperature (23 $^{\circ}$ C), before adding the substrate and ATP to the reaction. The 20 μ l kinase reaction consisted of the following: 4 μ l of test compound (10 μ M, 1% DMSO), 8 μ l of enzyme (8 ng *HsGSK-3 β* or 32 ng *PfGSK-3*) and 8 μ l of ATP/substrate mix (ATP: 10 μ M; substrate: 0.8 mg/ml for *HsGSK-3 β* or 0.6 mg/ml for *PfGSK-3*) in kinase reaction buffer. The reaction was incubated at 30 $^{\circ}$ C for 30 min and then equilibrated to room temperature for 30 min. 5 μ l of the kinase reaction was then transferred to a solid white 384-well plate (Brandplates $^{\circ}$; Merck, Darmstadt, Germany), 5 μ l of ADP-Glo $^{\text{TM}}$ Reagent was added, and incubated for 40 min at room temperature. 10 μ l of Kinase Detection Reagent was then added and incubated for 30 min at room temperature. Luminescence was measured using a SpectraMax $^{\circ}$ iD3 multi-mode microplate reader (integration time: 0.5 s per well), and the

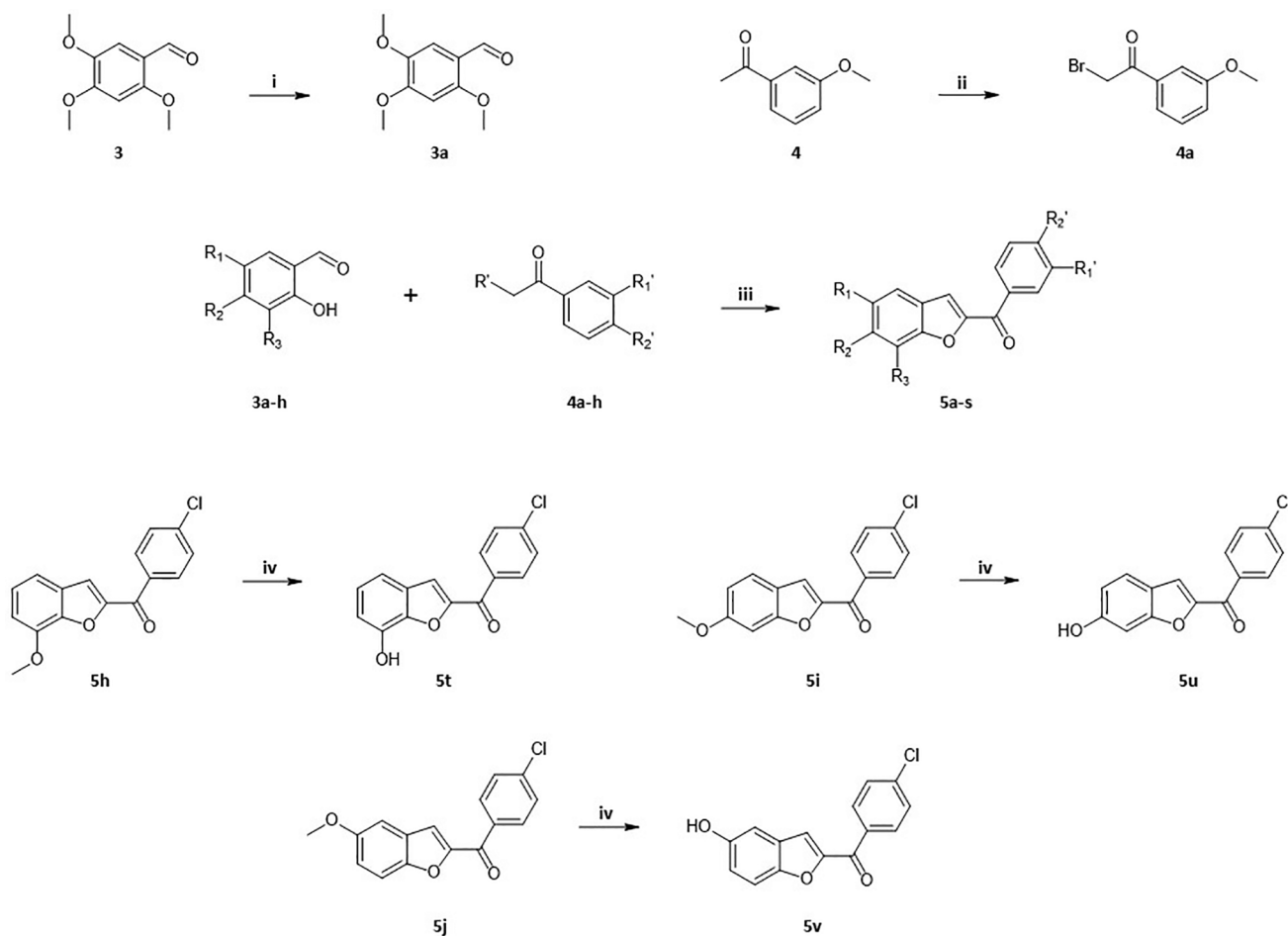
accompanying SoftMax Pro 7 software (Molecular Devices, San Jose, CA).

For compounds showing inhibitory activity at 10 μ M, dose-response curves were performed. Using Graphpad Prism Software, the sigmoidal dose-response curves were obtained by plotting luminescence against the logarithm of the compounds' concentrations. The IC $_{50}$ values were then calculated using nonlinear regression. All reactions were performed in triplicate, and data was normalised to a negative control (reaction without kinase). Indirubin-3'-monoxime, a known inhibitor of both *HsGSK-3 β* and *PfGSK-3* [18,25], was included as a positive control. The intra- and inter-assay CV values are available in the [Supplementary material](#) (Table A).

3. Results and discussion

3.1. Chemistry

Except for reagents **3a** and **4a**, all other reagents were purchased from commercial suppliers and were used as supplied. The reagents (**3a** & **4a**) and target compounds (**5a-v**) were synthesised according to the reactions shown in [Scheme 1](#). 2-Hydroxy-4,5-dimethoxybenzaldehyde (**3a**) was obtained by *ortho*-demethylation of 2,4,5-trimethoxybenzaldehyde using BBr $_3$ as demethylation agent in DCM [30]. The selective demethylation at the *ortho*-position is a result of the *ortho*-directing effect of the carbonyl group [31]. The selective α -bromination of 3'-methoxyacetophenone was achieved using CuBr $_2$ in ethyl acetate/DCM (1:1) to yield 2-bromo-3'-methoxyacetophenone (**4a**) [32,33]. Compounds **5a-v** were prepared using Rap-Stoermer condensation reaction



Scheme 1. Synthesis of reagents **3a** & **4a**, and compounds **5a-v**. Reagents and conditions: i) BBr $_3$, ice bath (10 min), room temperature (5 h); ii) CuBr $_2$, ethyl acetate/DCM (1:1), 85 $^{\circ}$ C (24 h); iii) K $_2$ CO $_3$, PEG-400, 100 $^{\circ}$ C (1–2 h); iv) AlCl $_3$, toluene, 100 $^{\circ}$ C (2–3 h).

between salicylaldehydes and α -haloketones in PEG-400 [34]. Compounds **5t-v** were prepared by demethylation of compounds **5h-j** with AlCl_3 in toluene [35].

Reagents and compounds were obtained in fair to good yields (42–91%), except for compounds **5t-v** which had poor yields (27–29%). The structures and purity of the target compounds were verified by ^1H NMR, ^{13}C NMR, MS, melting point and HPLC analyses.

3.2. Expression and purification of recombinant HsGSK-3 β and PfGSK-3

Recombinant HsGSK-3 β was expressed from pET32a(+) as a thioredoxin-histidine-fusion of approximately 64 kDa. Co-expression of the pGro7 chaperone proteins (*groES* and *groEL*) with recombinant HsGSK-3 β , facilitated the protein folding process and thereby increased the recovery of soluble HsGSK-3 β . The C-terminal histidine-tag allowed for easy detection and purification using nickel-affinity chromatography.

PfGSK-3 was expressed using a similar method to the one described by Droucheau and co-workers [18], however, the present study expressed the full length PfGSK-3 protein instead of a truncated version where the N-terminal is omitted. The pBAD/Thio-TOPO[®] system was used as it tightly regulates expression, thus preventing “leaky” expression of potentially toxic proteins such as PfGSK-3. The recombinant PfGSK-3 protein (approximately 68 kDa) was expressed with an N-terminal thioredoxin fusion protein for increased solubility, and a C-terminal histidine-tag for purification with nickel-affinity chromatography.

The PfGSK-3 protein required additional purification due to the presence of several other proteins that co-eluted with PfGSK-3 (Fig. 2). The washing protocol of the Protino[®] Ni-TED column was adapted as follows: instead of washing only with LEW buffer, the column was also washed with diluted Elution buffer (containing only 5% imidazole). As a result, some of the previously co-eluted proteins could be washed away before eluting the PfGSK-3 protein. As a second purification step, the Amicon[®] Ultra-15 centrifugal device was used to remove all proteins

smaller than 50 kDa. Despite the additional measures to purify the PfGSK-3 protein, an additional protein (>50 kDa) still remained. Droucheau and co-workers [18] also reported the presence of another protein after PfGSK-3 purification. They concluded that this additional protein was likely a proteolytic degradation product of PfGSK-3, and used the PfGSK-3 protein without further purification.

3.3. ADP-Glo[™] kinase assay

A series of benzofuran derivatives (**5a-v**) was screened against recombinant PfGSK-3 and HsGSK-3 β using the ADP-Glo[™] Kinase Assay. The compounds that showed inhibitory activity at a concentration of 10 μM , were evaluated further by determining the IC_{50} values (Table 1). Of the seven compounds that showed inhibitory activity during the initial screening, one compound was selective towards HsGSK-3 β (**5u**), one compound was unselective inhibiting both PfGSK-3 and HsGSK-3 β (**5v**), and five compounds were selective towards PfGSK-3 (**5k**, **5m**, **5p**, **5r**, **5s**).

Compound **5p** was the most active compound of the series with an IC_{50} value of 0.00049 μM and a 316-fold selectivity for PfGSK-3 versus HsGSK-3 β . This was closely followed by the activity of compound **5m** which exhibits an IC_{50} value of 0.00168 μM with a 175-fold selectivity towards PfGSK-3. Compared to the reference inhibitor, indirubin-3'-monoxime (IC_{50} : 0.250 μM), compound **5p** and **5m** are approximately 510-fold and 148-fold more potent, respectively. The most selective PfGSK-3 inhibitor of the series was compound **5r**, with a 559-fold selectivity for PfGSK-3 versus HsGSK-3 β . As mentioned previously, PfGSK-3 inhibitors would have to be very selective in order to prevent simultaneous inhibition of HsGSK-3 β and the possible ensuing side effects [21,22].

Comparing the activity of compound **5p** and **5m** to that of the 4-phenylthieno[2,3-*b*]pyridine inhibitors (**1** and **2**, Fig. 1), the benzofurans developed in this study were more potent PfGSK-3 inhibitors, demonstrating lower IC_{50} values than the 4-phenylthieno[2,3-*b*]

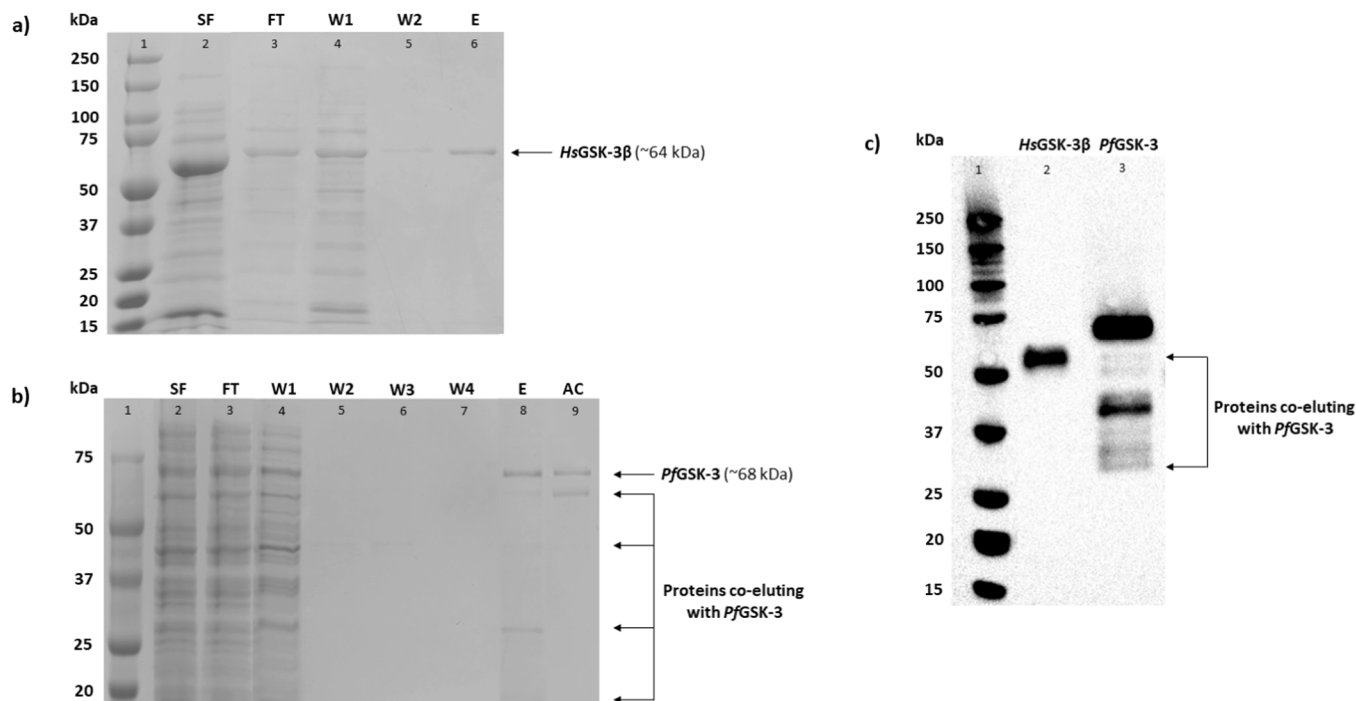
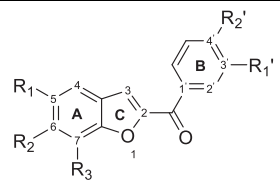


Fig. 2. 10% SDS-PAGE analysis of the different fractions collected during purification of recombinant HsGSK-3 β (a) and PfGSK-3 (b). For HsGSK-3 β (a): Lane 1: protein ladder (kDa); SF: soluble fraction loaded onto the Protino[®] Ni-TED column; W1-W2: column wash with LEW buffer; E: column elution fraction. For PfGSK-3 (b): Lane 1: protein ladder (kDa); SF: soluble fraction loaded onto the Protino[®] Ni-TED column; W1: column wash with LEW buffer; W2-W4: column wash with 5% imidazole buffer; E: column elution fraction; AC: concentrate collected from the Amicon[®] centrifugal device. Western blot analysis (c) of the column elution fractions of HsGSK-3 β and PfGSK-3.

Table 1
Structures and IC₅₀ values of benzofuran derivatives assayed against recombinant *HsGSK-3β* and *PfGSK-3*.



#	Ring A			Ring B		IC ₅₀ ± SD (μM) ^a		SI ^b
	5	6	7	3'	4'	<i>HsGSK-3β</i>	<i>PfGSK-3</i>	
	R ₁	R ₂	R ₃	R _{1'}	R _{2'}			
5a	H	H	H	H	H	–	–	–
5b	Cl	H	H	H	H	–	–	–
5c	Cl	H	Br	H	H	–	–	–
5d	Cl	H	H	H	Cl	–	–	–
5e	Cl	H	Br	H	Cl	–	–	–
5f	H	H	H	H	Cl	–	–	–
5g	H	Diethylamino	H	H	H	–	–	–
5h	H	H	OCH ₃	H	Cl	–	–	–
5i	H	OCH ₃	H	H	Cl	–	–	–
5j	OCH ₃	H	H	H	Cl	–	–	–
5k	H	OCH ₃	H	Cl	Cl	25.817 ± 0.354	1.692 ± 0.850	15
5l	H	OCH ₃	H	H	H	–	–	–
5m	H	OCH ₃	H	H	F	0.294 ± 0.014	0.00168 ± 0.00005	175
5n	H	OCH ₃	H	H	Br	–	–	–
5o	H	OCH ₃	H	H	OCH ₃	–	–	–
5p	H	OCH ₃	H	H	CN	0.155 ± 0.005	0.00049 ± 0.00010	316
5q	OCH ₃	OCH ₃	H	H	Cl	–	–	–
5r	H	OCH ₃	H	OCH ₃	H	70.997 ± 0.506	0.127 ± 0.010	559
5s	H	H	OCH ₃	OCH ₃	H	33.960 ± 1.054	0.440 ± 0.113	77
5t	H	H	OH	H	Cl	–	–	–
5u	H	OH	H	H	Cl	0.137 ± 0.002	12.560 ± 0.352	0
5v	OH	H	H	H	Cl	5.449 ± 0.170	5.103 ± 0.580	1
Indirubin-3'-monoxime						0.005 ± 0.001 (0.005–0.05) ^c	0.250 ± 0.080 (0.065) ^d	–

^a The IC₅₀ values were determined in triplicate and expressed as the mean ± standard deviation (SD) in μM. IC₅₀ values were only determined for those compounds that exhibited inhibitory activity during the initial screening at 10 μM concentration.

^b The selectivity index (SI) is the selectivity for *PfGSK-3* and is given as the ratio of (*HsGSK-3β* IC₅₀)/ (*PfGSK-3* IC₅₀).

^c Literature value obtained from [37] for recombinant *HsGSK-3β*.

^d Literature value obtained from [18] for a truncated form of recombinant *PfGSK-3*.

pyridines. However, as Masch and co-workers [29] pointed out, comparison of IC₅₀ values is only relevant when the same assay is used to generate the data. Fugel and co-workers [25] used a radiometric kinase assay, while Masch and co-workers [29] compared a radiometric assay to the Kinase-Glo® Plus Luminescent Assay (Promega, Madison, WI). Although, the ADP-Glo™ Kinase Assay used during this study is similar to the Kinase-Glo® Plus Assay, the two assays differ in that they quantify different aspects of the kinase reaction. The Kinase-Glo® Plus Assay quantifies the remaining ATP after the kinase reaction has taken place, and the resulting luminescent signal is inversely proportional to the kinase activity. The ADP-Glo™ Kinase Assay quantifies ADP generated during the kinase reaction, and the luminescent signal is directly proportional to the kinase activity. An advantage of the ADP-Glo™ Kinase Assay used in this study is that much lower levels of ADP formation can be detected, which is beneficial when working with low enzyme concentrations or kinases with a low enzyme turnover rate [36]. The choice of kinase assay is therefore an important aspect that should be carefully considered and standardised to enable comparison of the IC₅₀ values in future studies.

Analysing the structure-activity relationships (SARs) of the benzofuran derivatives with both *PfGSK-3* and *HsGSK-3β*, revealed some interesting trends. The *PfGSK-3* selective compounds (**5k**, **5m**, **5p**, **5r**, **5s**) all have a C6-OCH₃ substitution on ring A, except for compound **5s** which has a C7-OCH₃ substitution. Active compounds seem to favour the substitution of ring A with a single OCH₃ group at position C6, for when the position of the OCH₃ group is changed (**5j**: C5-OCH₃) or an additional OCH₃ group is added to ring A (**5q**: C5,6-diOCH₃), the compound

loses its activity. Likewise, when substituents other than OCH₃ are present at position C6 of ring A, the compound either loses its activity (**5g**: C6-diethylamino group), or becomes more selective towards *HsGSK-3β* (**5u**: C6-OH). A loss of activity is also observed when ring A is substituted with Cl and Br groups (**5b** & **5d**: C5-Cl; **5c** & **5e**: C5-Cl, C7-Br), or when ring A is unsubstituted (**5a** & **5f**). Substituting ring A with an OH group results in unselective activity (**5v**: C5-OH) or loss of activity (**5t**: C7-OH).

The activity of the compounds also seems to be influenced by the substitution pattern of ring B. The compounds with C6-OCH₃ substitution on ring A are active and selective towards *PfGSK-3* when ring B is substituted with a C3',4'-diCl (**5k**); C4'-F (**5m**); C4'-CN (**5p**); or C3'-OCH₃ (**5r**) group. However, when ring B is unsubstituted (**5l**) or substituted with a Cl (**5i**), Br (**5n**) or OCH₃ (**5o**) group at position C4', the compounds were inactive. Likewise, the activity of compounds with C7-OCH₃ substitution on ring A is also influenced by the substitution pattern of ring B. This is clearly demonstrated when comparing compounds **5s** and **5h**. The *PfGSK-3* selective compound **5s** is substituted at position C3' (OCH₃ group) of ring B, while the inactive compound **5h** is substituted at position C4' (Cl group). The effect of substituting ring B with other types of substituents at position C3' and C4' still has to be determined.

4. Conclusion

With the continuing threat of multi-drug resistant malaria, an urgent need exists to develop novel antimalarial drugs. Herein, a series of

benzofuran derivatives was evaluated as potent and selective PfGSK-3 inhibitors. Five compounds demonstrated selectivity for PfGSK-3 over HsGSK-3 β , with IC₅₀ values ranging from 0.00049 to 1.692 μ M. Compound **5p** and **5m** were the most potent PfGSK-3 inhibitors of the series (IC₅₀: 0.00049 μ M and 0.00168 μ M, respectively), while compound **5r** was the most selective inhibitor with a 559-fold selectivity towards PfGSK-3. The SARs of these compounds provide valuable insight with regards to the use of chalcone-based scaffolds for the design of PfGSK-3 selective inhibitors. The results warrant further exploration of the benzofuran class of inhibitors with regards to their interaction with the PfGSK-3 active site (molecular docking), *in vitro* activity against blood stage *P. falciparum* parasites, toxicity, and selectivity towards other human protein kinases.

Declaration of Competing Interest

The authors declare that they have no known competing financial interests or personal relationships that could have appeared to influence the work reported in this paper.

Acknowledgements

Financial support for this study was provided by the North-West University and the National Research Foundation (NRF) of South Africa (Grant number: 112535). The authors wish to thank Dr. D. Otto and Dr. J. Jordaan of Chemical Research Beneficiation (NWU) for NMR and MS analyses, respectively. We also wish to thank Prof. J. du Preez for his assistance with the HPLC analyses, and Prof. O. Thekiso for use of the SpectraMax plate reader.

Appendix A. Supplementary material

Supplementary data to this article can be found online at <https://doi.org/10.1016/j.bioorg.2021.104839>.

References

- [1] K.S. Bhullar, N.O. Lagaron, E.M. McGowan, I. Parmar, A. Jha, B.P. Hubbard, H.P. V. Rupasinghe, Kinase-targeted cancer therapies: progress, challenges and future directions, *Mol. Cancer* 17 (2018) 48–67, <https://doi.org/10.1186/s12943-018-0804-2>.
- [2] R. Kannaiyan, D. Mahadevan, A comprehensive review of protein kinase inhibitors for cancer therapy, *Expert Rev. Anticancer Ther.* 18 (2018) 1249–1270, <https://doi.org/10.1080/14737140.2018.1527688>.
- [3] A. Altman, K.F. Kong, Protein kinase C inhibitors for immune disorders, *Drug Discov. Today* 19 (2014) 1217–1221, <https://doi.org/10.1016/j.drudis.2014.05.008>.
- [4] M. Rask-Andersen, J. Zhang, D. Fabbro, H.B. Schioth, Advances in kinase targeting: current clinical use and clinical trials, *Trends Pharmacol. Sci.* 35 (2014) 604–620, <https://doi.org/10.1016/j.tips.2014.09.007>.
- [5] J.A. Whang, B.Y. Chang, Bruton's tyrosine kinase inhibitors for the treatment of rheumatoid arthritis, *Drug Discov. Today* 19 (2014) 1200–1204, <https://doi.org/10.1016/j.drudis.2014.03.028>.
- [6] M.J. Gardner, N. Hall, E. Fung, O. White, M. Berriman, R.W. Hyman, J.M. Carlton, A. Pain, K.E. Nelson, S. Bowman, I.T. Paulsen, K. James, J.A. Eisen, K. Rutherford, S.L. Salzberg, A. Craig, S. Kyes, M.S. Chan, V. Nene, S.J. Shallom, B. Suh, J. Peterson, S. Angiuoli, M. Peretea, J. Allen, J. Selengut, D. Haft, M.W. Mather, A. B. Vaidya, D.M. Martin, A.H. Fairlamb, M.J. Fraunholz, D.S. Roos, S.A. Ralph, G. I. McFadden, L.M. Cummings, G.M. Subramanian, C. Mungall, J.C. Venter, D. J. Carucci, S.L. Hoffman, C. Newbold, R.W. Davis, C.M. Fraser, B. Barrell, Genome sequence of the human malaria parasite *Plasmodium falciparum*, *Nature* 419 (2002) 498–511, <https://doi.org/10.1038/nature01097>.
- [7] D.G. Cabrera, A. Horatscheck, C.R. Wilson, G. Basarab, C.J. Eyermann, K. Chibale, Plasmodial kinase inhibitors: license to cure? *J. Med. Chem.* 61 (2018) 8061–8077, <https://doi.org/10.1021/acs.jmedchem.8b00329>.
- [8] F. Canduri, P.C. Perez, R.A. Caceres, W.F. de Azevedo, Protein kinases as targets for antiparasitic chemotherapy drugs, *Curr. Drug Targets* 8 (2007) 389–398, <https://doi.org/10.2174/138945007780058979>.
- [9] C. Doerig, Protein kinases as targets for anti-parasitic chemotherapy, *Biochim. Biophys. Acta* 1697 (2004) 155–168, <https://doi.org/10.1016/j.bbapap.2003.11.021>.
- [10] C. Doerig, O. Billker, T. Haystead, P. Sharma, A.B. Tobin, N.C. Waters, Protein kinases of malaria parasites: an update, *Trends Parasitol.* 24 (2008) 570–577, <https://doi.org/10.1016/j.pt.2008.08.007>.
- [11] C. Doerig, O. Billker, D. Pratt, J. Endicott, Protein kinases as targets for antimalarial intervention: kinomics, structure-based design, transmission-blockade, and targeting host cell enzymes, *Biochim. Biophys. Acta* 1754 (2005) 132–150, <https://doi.org/10.1016/j.bbapap.2005.08.027>.
- [12] WHO (World Health Organization), World Malaria Report 2019. https://www.who.int/malaria/publications/world_malaria_report/en/, 2019 (accessed 17 February 2020).
- [13] S. Dhiman, Are malaria elimination efforts on right track? An analysis of gains achieved and challenges ahead, *Infect. Dis. Poverty* 8 (2019) 14, <https://doi.org/10.1186/s40249-019-0524-x>.
- [14] S. Rout, R.K. Mahapatra, *Plasmodium falciparum*: multidrug resistance, *Chem. Biol. Drug Des.* 93 (2019) 737–759, <https://doi.org/10.1111/cbdd.13484>.
- [15] A. Uwimana, E. Legrand, B.H. Stokes, J.M. Ndikumana, M. Warsame, N. Umulisa, D. Ngamije, T. Munyaneza, J.B. Mazarati, K. Munguti, P. Campagne, A. Criscuolo, F. Ariey, M. Murindahabi, P. Ringwald, D.A. Fidock, A. Mbituyumuremyi, D. Menard, Emergence and clonal expansion of *in vitro* artemisinin-resistant *Plasmodium falciparum* kelch13 R561H mutant parasites in Rwanda, *Nat. Med.* 26 (2020) 1602–1608, <https://doi.org/10.1038/s41591-020-1005-2>.
- [16] L. Solyakov, J. Halbert, M.M. Alam, J.P. Semblat, D. Dorin-Semblat, L. Reininger, A.R. Bottrill, S. Mistry, A. Abdi, C. Fennell, Z. Holland, C. Demarta, Y. Bouza, A. Sicard, M.P. Nivez, S. Eschenlauer, T. Lama, D.C. Thomas, P. Sharma, S. Agarwal, S. Kern, G. Pradel, M. Graciotti, A.B. Tobin, C. Doerig, Global kinomic and phospho-proteomic analyses of the human malaria parasite *Plasmodium falciparum*, *Nat. Commun.* 2 (2011) 565, <https://doi.org/10.1038/ncomms1558>.
- [17] P. Ward, L. Equinet, J. Packer, C. Doerig, Protein kinases of the human malaria parasite *Plasmodium falciparum*: the kinome of a divergent eukaryote, *BMC Genomics* 5 (2004) 79, <https://doi.org/10.1186/1471-2164-5-79>.
- [18] E. Droucheau, A. Primot, V. Thomas, D. Mattei, M. Knockaert, C. Richardson, P. Sallicandro, P. Alano, A. Jafarshad, B. Baratte, C. Kunick, D. Parzy, L. Pearl, C. Doerig, L. Meijer, *Plasmodium falciparum* glycogen synthase kinase-3: molecular model, expression, intracellular localisation and selective inhibitors, *Biochim. Biophys. Acta* 1697 (2004) 181–196, <https://doi.org/10.1016/j.bbapap.2003.11.023>.
- [19] R. Dajani, E. Fraser, S.M. Roe, N. Young, V. Good, T.C. Dale, L.H. Pearl, Crystal structure of glycogen synthase kinase 3 β : Structural basis for phosphate-primed substrate specificity and autoinhibition, *Cell* 105 (2001) 721–732, [https://doi.org/10.1016/s0092-8674\(01\)00374-9](https://doi.org/10.1016/s0092-8674(01)00374-9).
- [20] E. Beurel, S.F. Grieco, R.S. Jope, Glycogen synthase kinase-3 (GSK3): regulation, actions, and diseases, *Pharmacol. Ther.* 148 (2015) 114–131, <https://doi.org/10.1016/j.pharmthera.2014.11.016>.
- [21] S. Lovestone, M. Boada, B. Dubois, M. Hüll, J.O. Rinne, H.J. Huppertz, M. Calero, M.V. Andrés, B. Gómez-Carrillo, T. León, T. del Ser, A Phase II Trial of Tideglusib in Alzheimer's Disease, *J. Alzheimers Dis.* 45 (2015) 75–88, <https://doi.org/10.3233/JAD-141959>.
- [22] A. Martinez, C. Gil, D.I. Perez, Glycogen synthase kinase 3 inhibitors in the next horizon for Alzheimer's disease treatment, *Int. J. Alzheimers Dis.* 2011 (2011), 280502, <https://doi.org/10.4061/2011/280502>.
- [23] G.V. Rayasam, V.K. Tulasi, R. Sodhi, J.A. Davis, A. Ray, Glycogen synthase kinase 3: more than a namesake, *Br. J. Pharmacol.* 156 (2009) 885–898, <https://doi.org/10.1111/j.1476-5381.2008.00085.x>.
- [24] S.S. Ebadat, M.H. Linh, A. Longeon, N.J. de Voogd, E. Durieu, L. Meijer, M. L. Bourguet-Kondracki, A.N. Singab, W.E. Muller, P. Proksch, Dispacamide E and other bioactive bromopyrrole alkaloids from two Indonesian marine sponges of the genus *Stylisha*, *Nat. Prod. Res.* 29 (2015) 231–238, <https://doi.org/10.1080/14786419.2014.947496>.
- [25] W. Fugel, A.E. Oberholzer, B. Gschloessl, R. Dzikowski, N. Pressburger, L. Preu, L. H. Pearl, B. Baratte, M. Ratin, I. Okun, C. Doerig, S. Kruggel, T. Lemcke, L. Meijer, C. Kunick, 3,6-Diamino-4-(2-halophenyl)-2-benzoylthieno[2,3-b]pyridine-5-carbonitriles are selective inhibitors of *Plasmodium falciparum* glycogen synthase kinase-3, *J. Med. Chem.* 56 (2013) 264–275, <https://doi.org/10.1021/jm301575n>.
- [26] A. Masch, C. Kunick, Selective inhibitors of *Plasmodium falciparum* glycogen synthase-3 (PfGSK-3): New antimalarial agents? *Biochim. Biophys. Acta* 2015 (1854) 1644–1649, <https://doi.org/10.1016/j.bbapap.2015.03.013>.
- [27] S. Kruggel, T. Lemcke, Comparative investigation of the ATP-binding site of human and plasmodial glycogen synthase kinase-3, *QSAR Comb. Sci.* 28 (2009) 885–890, <https://doi.org/10.1002/qsar.200860193>.
- [28] D.I. Osolodkin, N.V. Zakharevich, V.A. Palyulin, V.N. Danilenko, N.S. Zefirov, Bioinformatic analysis of glycogen synthase kinase 3: human versus parasite kinases, *Parasitology* 138 (2011) 725–735, <https://doi.org/10.1017/s0031182011000151>.
- [29] A. Masch, A. Nasereddin, A. Alder, M.J. Bird, S.I. Schweda, L. Preu, C. Doerig, R. Dzikowski, T.W. Gilberger, C. Kunick, Structure-activity relationships in a series of antiplasmodial thieno[2,3-b]pyridines, *Malar. J.* 18 (2019) 89, <https://doi.org/10.1186/s12936-019-2725-y>.
- [30] D.R. Laplace, B. Verbraken, K. Van Hecke, J.M. Winne, Total synthesis of (+/-)-fronodosin B and (+/-)-5-epi-liphagal by using a concise (4+3) cycloaddition approach, *Chem. Eur. J.* 20 (2014) 253–262, <https://doi.org/10.1002/chem.201303273>.
- [31] K. Lal, S. Ghosh, R.G. Salomon, Hydroxyl-directed regioselective monodemethylation of polymethoxyarenes, *J. Org. Chem.* 52 (1986) 1072–1078.
- [32] E. Bellale, M. Naik, B.V. V, A. Ambady, A. Narayan, S. Ravishankar, V. Ramachandran, P. Kaur, R. McLaughlin, J. Whiteaker, S. Morayya, S. Guptha, S. Sharma, A. Raichurkar, D. Awasthy, V. Achar, P. Vachaspati, B. Bandodkar, M. Panda, M. Chatterji, Diarylthiazole: an antimycobacterial scaffold potentially targeting PrfB-PrfA two-component system, *J. Med. Chem.* 57 (2014) 6572–6582, <https://doi.org/10.1021/jm500833f>.

- [33] L.C. King, G.K. Ostrum, Selective bromination with copper (II) bromide, *J. Org. Chem.* 29 (1964) 3459–3461.
- [34] S. Zhao, X. Wang, L. Zhang, Polyethylene glycol (PEG-400) as an efficient and recyclable reaction medium for the synthesis of 2-arylbenzofurans, *Org. Prep. Proced. Int.* 45 (2013) 421–428, <https://doi.org/10.1080/00304948.2013.816214>.
- [35] L.J. Legoabe, A. Petzer, J.P. Petzer, α -Tetralone derivatives as inhibitors of monoamine oxidase, *Bioorg. Med. Chem. Lett.* 24 (2014) 2758–2763, <https://doi.org/10.1016/j.bmcl.2014.04.021>.
- [36] C. Tanega, M. Shen, B.T. Mott, C.J. Thomas, R. MacArthur, J. Inglese, D.S. Auld, Comparison of bioluminescent kinase assays using substrate depletion and product formation, *Assay Drug Dev. Technol.* 7 (2009) 606–614, <https://doi.org/10.1089/adt.2009.0230>.
- [37] S. Leclerc, M. Garnier, R. Hoessel, D. Marko, J.A. Bibb, G.L. Snyder, P. Greengard, J. Biernat, Y.Z. Wu, E.M. Mandelkow, G. Eisenbrand, L. Meijer, Indirubins inhibit glycogen synthase kinase-3 beta and CDK5/p25, two protein kinases involved in abnormal tau phosphorylation in Alzheimer's disease. A property common to most cyclin-dependent kinase inhibitors? *J. Biol. Chem.* 276 (2001) 251–260, <https://doi.org/10.1074/jbc.M002466200>.